CLM-P599

CLM-P599

UKAEA

Preprint

PARTICLE CONFINEMENT SCALING EXPERIMENTS IN THE CULHAM LEVITRON

T. EDLINGTON
W. H. W. FLETCHER
A. C. RIVIERE
T. N. TODD

CULHAM LABORATORY
Abingdon Oxfordshire

1980

CLM-P 599

PARTICLE CONFINEMENT SCALING EXPERIMENTS IN THE CULHAM LEVITRON

by

T Edlington, W H W Fletcher, A C Riviere,
T N Todd

Culham Laboratory, Abingdon, Oxon OX14 3DB, UK.

ABSTRACT

Experiments are described which investigate the parametric variation of particle confinement in heated and unheated decaying plasmas in the Culham Superconducting Levitron. The parameter range investigated, expressed in terms of a collisionality parameter is similar to that found in the current generation of reverse field pinch experiments and in the edge regime of present day tokamak experiments. The variation of the particle confinement time with electron temperature, electron density and magnetic field strength was found to be approximately of the form $\tau_p \propto \frac{T^{\frac{1}{2}} B^2}{n}$ which is that expected for classical diffusion ($D_{cl} \sim \nu_{ei} \cdot a_e^2$). However the measured confinement times were shorter than those predicted by classical diffusion by a factor of 3-10 depending on the magnetic shear. The diffusion rate was found to be approximately proportional to $\bar{L}_s^{-1.6}$ where $\bar{L}_s$ is the mean shear length. Low frequency spectra of floating potential fluctuations were measured and it was found that the amplitude of these fluctuations was reduced by increasing magnetic shear. The resistive-g mode has been suggested[1] as a possible explanation for the low frequency fluctuations and the diffusion coefficient predicted for this mode ($D = \gamma/k^2$) has a scaling similar to that observed.

(Submitted for publication in Nuclear Fusion)

May 1980

1. INTRODUCTION

Multipole experiments have in general achieved their main objective of demonstrating MHD stability [2]. As a result they have proved useful devices in which to study diffusion phenomena in experiments where the important parameters are under the control of the experimentalist. However even in these highly stable configurations only rarely [3] has classical diffusion been observed. Generally the confinement in these experiments has fallen short of this ideal. The mechanisms suggested to explain the additional diffusion include loss to mechanical supports [4], magnetic field errors, [5,17] ion-molecular reactions [6], convective cells [7] and electron density fluctuations [8]. However in many of the experiments it has proved difficult to isolate a single mechanism as being responsible for the diffusion. Experimental determination of the scaling of the diffusion is of considerable value when comparing the various theoretical options. In this paper the scaling of the diffusion observed in the Culham Levitron is described.

Several scaling laws for diffusion have been found in the various regimes in which multipole experiments have operated. Classical and vortex [9] diffusion ($D_\perp \propto n^{-\frac{1}{2}}$, independent of B) were reported on the Wisconsin Octupole [10,11] In the G A Octupole experiment in collisionless plasmas three distinct regimes were observed [12]. Neo-classical diffusion ($\tau_p \propto \frac{T_e^{\frac{1}{2}} B_p^2}{n}$) was observed when trapped electrons were significant. At lower densities diffusion attributed to thermal equilibrium fluctuations [13] was observed with $\tau_p \propto \frac{n_e^{\frac{1}{2}} M^{\frac{1}{2}}}{T_e^{\frac{1}{2}}}$. A third diffusion scaling law ($\tau_p \propto \frac{B_p}{T_e}$), the so-called poloidal Bohm scaling, was observed when the electron temperature was raised. At Princeton in the LSP and FM1 spherators a low temperature regime was observed [14] where the diffusion scaled pseudo-classically [15]. However above a certain density-dependent threshold in electron temperature the scaling became Bohm-like with a confinement time approximately 300 times the Bohm time ($D_B = \frac{1}{16} \frac{kT_e}{eB}$).

In this paper experimental results are presented which indicate that the

scaling law for particle confinement (energy confinement is believed to be dominated by the neutral gas) at low temperatures has a classical-like form similar to that observed in the low temperature regime in FM1. However the dependence on magnetic shear is found to be stronger [16] and up to electron temperatures of 2eV no evidence of Bohm scaling has been found. Vortex diffusion is expected to be small in the Levitron because of the strong shear and neo-classical effects are small since $B_p >> B_\phi$. The formation of magnetic islands or, in the extreme, ergodicity of field lines can enhance diffusion by increasing the effective step length for collisional diffusion processes. Calculation of magnetic field errors due to stabilising fields, ring tilt and high order asymmetries has shown that these effects may be important near the edge of the plasma, particularly at high toroidal fiels, but are not strong enough to explain the anomalous diffusion.

2. EXPERIMENTAL PROCEDURE

A detailed description of the Culham Levitron can be found elsewhere [18]. The device is an axisymmetric toroidal system with the main (poloidal) field produced by a fully levitated superconducting ring (major radius 30cm, minor radius 4.7cm). The shape of the magnetic flux surfaces is determined by superconducting vertical field coils. The shear can be varied by changing the current in a 72 turn winding which produces the toroidal magnetic field. The ratio of the total current in the toroidal winding to that in the ring, $\frac{I_z}{I_R}$, is approximately proportional to the inverse of the shear length L_s averaged around a magnetic flux surface. The plasma is produced by electron cyclotron resonance heating at microwave frequencies of 10, 16 and 30GHz. Resonant magnetic fields for these frequencies at approximately 1.5cm from the ring are 3.57, 5.8 and 10.7 kgauss and the corresponding ring currents are 110, 180 and 330 kA respectively.

The electron density at equilibrium and in the afterglow was measured with a 4mm microwave interferometer. The average electron temperature is

determined from absolute intensity measurements of the helium spectral line at 5876Å. In the main discharge a double Langmuir probe was used to measure the electron density and temperature profiles. Density and temperature profiles were also obtained in the decay using a multiple shot technique with the probe at a fixed position for each shot. The profiles were then reconstructed taking data at fixed times after the microwave heating was switched off. Where a confinement time τ_p is quoted it is taken from the decay rate of the mean electron density and the value was obtained without probes inserted into the plasma. Partial pressures of the main gases in the vacuum vessel were measured with mass spectrometers. Fluctuations in floating potential have been observed in the heated decays. These fluctuations were measured with a high impedance probe with a diameter of 0.6mm. The dominant low frequency components are damped by increasing magnetic shear and this suggests a possible link between the fluctuations and the diffusion.

In unheated decays at high neutral densities the electron cooling rate is so rapid that the electron temperature falls very rapidly to a low value $\sim$ 0.1eV whilst the electron density is still high. Under these conditions recombination becomes important as an electron loss mechanism. This is observed spectroscopically as an increase in light emission in the afterglow due to recombination mechanisms populating excited states of helium neutrals. For the experiments reported here recombination effects were kept small, either by having a relatively low background gas pressure ($\sim 2 \times 10^{-6}$ torr) or by supporting the electron temperature with non-resonant microwave heating.

3. EXPERIMENTAL RESULTS

1) Scaling with n_e and T_e

With a ring current of 110 kA, microwaves at 16 GHz have no fundamental resonance inside the plasma volume. Microwaves at this frequency were

therefore used as non-localised heating to maintain the electron temperature in the decay at a constant low value of approx. 1 eV. The profiles remain virtually flat for 100-150msec after the main heating is switched off but as the density decays the heating becomes strongly localised near the region of the 2nd harmonic of the electron cyclotron resonance. The electron temperature is sufficiently low that corrections to τ_p for ionisation can be neglected. The data from three heated decays with different values of I_z/I_R is summarised in Figure 1. The data is plotted only in the region where the electron temperature is approximately constant and in this region the confinement time is clearly proportional to the reciprocal of electron density. The electron temperature could not be varied sufficiently in these experiments to establish a scaling law.

In decays where non-resonant heating was not used scaling experiments were more difficult to interpret because the electron temperature varied rapidly. For these decays the rate equations for electron and ion temperature and electron density were used to model the particle and energy balance in the decaying plasma. The model used is summarised below by three coupled differential equations. No term has been included for thermal conductivity effects. Calculations using classical thermal conductivity suggest that such a term would be negligibly small in comparison to the strong electron-ion coupling and charge exchange losses.

$$\frac{dT_e}{dt} = -1.2 \times 10^{-8} \frac{(T_e - T_i) n_e}{T_e^{3/2}} - n_o E_{iloss} + 5.4 \times 10^{-27} \frac{n_e^2}{T_e^{3.8}} \quad \ldots (1)$$

$$\frac{dT_i}{dt} = 1.2 \times 10^{-8} \frac{(T_e - T_i) n_e}{T_e^{3/2}} - n_o (T_i - T_{gas})(\langle\sigma v\rangle_{cx} + \langle\sigma v\rangle_{ion}) \quad \ldots (2)$$

$$\frac{dn_e}{dt} = -\frac{5.1 \times 10^{-7}}{I_R^2} \frac{n_e^2}{T_e^{1/2}} + n_e n_o \langle\sigma v\rangle_{ion} - 2.7 \times 10^{-27} \frac{n_e^3}{T_e^{4.8}} \quad \ldots (3)$$

In Eqn.(1) classical electron-ion coupling is the main energy loss for electrons. In addition energy losses due to ionisation and excitation (E_{iloss}) at high temperatures are included and at low temperatures heating due to recombination is also allowed for. Energy is lost from the ions (Eqn.(2)) mainly by charge-exchange. The particle balance equation (3) includes an assumption about the form of the electron diffusion rate (the first term on the right hand side). Numerical solution of these equations using experimentally determined initial values of n_e and T_e predicts the electron temperature and density decay rates as a function of time. The actual form of the electron diffusion term was established by comparing the predictions of the code with the observed density decay. Figure 2 shows the degree of agreement obtained by assuming that the electron diffusion term is that shown in equation (3). This dependence on electron temperature, density and magnetic field is the same as for classical collisional diffusion. A classical confinement time[19] was estimated from electron temperature and density profiles measured 25 msec after the heating was switched off. The actual classical confinement time could be obtained from a 1-D numerical solution of the continuity equation in flux co-ordinates. However a reasonable estimate can be obtained by assuming that the confinement time for particles inside a flux surface is not a function of the distance of the flux surface from the ring.

Then since $\frac{\partial n}{\partial t} = - \underline{\nabla} \cdot \Gamma$

$$\int_{r_o}^{r} \frac{1}{n} \frac{\partial n}{\partial t} \, nr\partial r = - \int_{r_o}^{r} \partial (r\Gamma)$$

$$\therefore \quad \tau_{P_{class}} \approx \frac{\int_{ro}^{r} nrdr}{r\Gamma_{class}} \qquad (4)$$

The classical flux Γ_{class} was calculated from the profile measurements

using the relation $\Gamma_{class} = \nu_{ei}\, a_e^2 \left[- \left(1+\frac{T_e}{T_i}\right) \nabla n_e - \frac{n_e}{T_e} \nabla T_i + \frac{1}{2} \frac{n_e}{T_e} \nabla T_e \right]$. Although equation (4) is expressed in cylindrical geometry the calculation was done in flux geometry with the appropriate flux surface averaging. r_o was taken to be the peak of the density profile. The derived value of $\tau_{P_{class}}$ varied slightly with radius but the average value of 800msec is considerably longer than the observed confinement time. The calculated curves in Figure 2 were obtained by assuming diffusion occurs with a classical parametric dependence but with a rate 7 times faster than classical.

2) Scaling with Magnetic Field

Following the scaling arguments of Connor and Taylor[20] for a low β collisional plasma, if the flux Γ is a function only of n_e, T_e and B and a where a is a characteristic length, then dimensional constraints require that if $\tau_p \propto \frac{T_e^{\frac{1}{2}}}{n_e}$ as suggested above and $\tau_p = \frac{na}{\Gamma}$ then $\tau_p \propto a^2 B^2$. In the Levitron where the poloidal field is dominant, the average magnetic field is approximately proportional to the ring current. Confinement times from decays with different ring currents but with the ratio $\frac{I_z}{I_R}$ held constant are plotted in Figure 3. The ring current was varied between 110 kA and 330 kA and the data is normalised to a ring current of 120 kA assuming a classical B^2 variation of confinement time with average magnetic field. It is evident from Figure 3 that the data can be described by a single scaling law. When the dependence on electron density and temperature is allowed for the confinement time is found to increase as the square of the mean magnetic field.

3) Scaling with Shear

It is clear from Figure 1 that the particle confinement time is strongly dependent on the ratio of $\frac{I_z}{I_R}$. The scaling from the data in Figure 1 is

approximately $\tau_p \propto \frac{1}{L_s^2} \propto \left(\frac{I_z}{I_R}\right)^2$. In Figure 4, data from unheated decays indicates a similar relation between confinement and shear at constant electron density and temperature, although at temperatures lower than those shown the scaling is less strong. The effect of recombination at the lower temperatures is not sufficient to explain this discrepancy. Figure 5 summarises all the data shown in Figure 1 and Figure 4, including data from decays at higher ring currents and clearly shows a consistent improvement in confinement with increasing shear. A best numerical fit to the data gives a scaling $\tau \propto {}^{1}/_{L_s}{}^{1.6}$.

4) Potential Fluctuations

A high impedance probe at a fixed radial position was used to measure fluctuations in floating potential ($\tilde{\phi}$) as a function of time. Ellis and Motley have pointed out[22] that some part of floating potential fluctuations can be caused by fluctuations in electron temperature. The size of this effect is not known for these measurements. The signals were recorded on magnetic tape along with the probe position and later digitised and Fourier analysed on a local computer[21]. The power spectra for two values of toroidal field are shown in Figure 6 where the ring current was 110 kA and the electron temperature was supported by 16 GHz non-resonant heating. The data was taken on the outer density gradient at a distance of 3.25 cm from the ring surface and was obtained by sampling the a.c.voltage for 5 msec approximately 20 msec after the ECRH was switched off. The strong low frequency group is clearly reduced in amplitude as the toroidal field is increased.

4. DISCUSSION

We have reported previously[1] on the observations of low frequency potential fluctuations in ECRH discharges. In the afterglow the fluctuations have a low amplitude but in the heated decays the levels are measurable and,

at low toroidal fields, values of $\frac{e\tilde{\phi}}{kT_e}$ comparable with those in the main discharge are observed. In [1] several different theoretical alternatives were discussed to explain the radial dependence and shear scaling of the observed fluctuations. The resistive-g mode seemed most likely to explain the experimental results and the measured diffusion was compared with that predicted by a linear theory of this mode in slab geometry. In both the limits of strong and weak shear the diffusion predicted by this model (based on $D = \gamma/k_x^2$) has the form $D \propto L_s^2 \nu_{ei} a_e^2$ where ν_{ei} is the electron-ion collision frequency and a_e is the electron gyroradius. The growth rate can be obtained by solving the eigenvalue equation for ω given in [1].

$$(\omega + \omega_D)^2(\omega + \omega_{*e}/\tau) \left\{ \omega - \omega_{*e}(1 + 1.7\eta_e) \right\} = - \frac{i L_s^2 \nu_{ei} \omega}{(2n+1)k_y^2 a_i^2 V_{TE}}$$

$$\times \left[\omega_{*e}\omega_p/\tau + k_y^2 a_i^2/(\omega + \omega_D)(\omega + \omega_{*e}/\tau) \right]^2$$

where $\tau = \frac{T_e}{T_i}$.

This equation has been solved numerically using density and temperature profiles measured in the decay and shown in fig.7. The result of this analysis is shown in Figure 8 where the calculated growth rate and radial width of the n = 0, m = 1 mode have been used to give a value for the diffusion coefficient based on the quasilinear relation $D = \gamma/k_x^2$ and including only the n = 0, m = 1 mode. The strong shear dependence observed experimentally is clearly predicted by this theoretical model. The measured confinement times were compared to the average values of D predicted by the model by assuming $\tau_p = \frac{2.89}{D}$. The characteristic scale length of 1.7cm used here is derived from the results of a 1-D classical transport code. The predicted diffusion is approximately ten times larger than the observed diffusion. A similar ratio was obtained for the measurements in the main discharge[1]. This quasi-linear estimate of the diffusion can only be regarded as an upper limit and we make this estimate only to demonstrate that the mode can generate sufficient transport to explain the observations.

5. SUMMARY

A single empirical scaling law for particle confinement ($\tau_p \propto n_e^{\alpha} T_e^{\beta} B^{\gamma} L_s^{\delta}$) has been experimentally established for both heated and unheated decays in the Culham Levitron. A numerical "best fit" to all the data available gives $\alpha = -1.05$, $\beta = 0.55$, $\gamma = 1.7$, $\delta = -1.6$. The confinement time has a classical-like dependence on electron density, electron temperature and magnetic field. However the rate of diffusion is anomalously high at low shear and is strongly damped by increasing magnetic shear. A theoretical model of the resistive-g mode, used previously [1] to explain the diffusion in the main discharge has been applied to the decay and satisfactory agreement achieved between the predicted and the observed scaling of the confinement time. The growth rate for this mode in the decay has been calculated and the quasi-linear prediction of the diffusion is larger than that observed.

6. ACKNOWLEDGEMENTS

The authors gratefully acknowledge the considerable contribution of the whole Levitron experimental team led by Dr D R Sweetman. In particular, the authors would like to thank Dr J G Cordey, Mr M W Alcock, Mr N R Ainsworth and Mr M F Payne. The cooperation and hard work of the Levitron operating team led by Mr R E Bradford was also essential.

REFERENCES

1. N R Ainsworth et al. Proc. 7th Int.Conf. on Plasma Physics and Contr.Nucl. Fusion Research, Innsbruck, Austria (1978). Vol.1, pp.745-761.

2. S Yoshikawa, Nuclear Fusion 13 (1973) 433.

3. G A Navratil and R S Post, Physics Letters 64A (1977) 223.

4. R Freeman, M Okabayashi, G Pacher, B Ripin, J A Schmidt, J Sinnis, S Yoshikawa. Proc.Conf.on Plasma Physics and Controlled Nuclear Fusion Research, 1 (1971) 27.

5. M Okabayashi and R Freeman, Phys. Fluids 15 (1972) 1346.

6. B H Ripin, M Okabayashi, J Schmidt, V Voitsenja, S Yoshikawa. Phys.Rev. Letts. 28 (1972) 138.

7. J Schmidt Phys. Rev. Lett. 24 (1970) 721

8. N R Ainsworth et al. Proc. 7th Eur.Conf. on Contr.Fus. and Plasma Phys. Lausanne (1975),Vol.2, pp 127-136.

9. H Okuda, J M Dawson, Phys.Rev.Lett.28 (1972) 1625.

10. G A Navratil, R Post and A Butcher Ehrhardt, Phys.Fluids 20 (1977) 156.

11. J R Drake, J R Greenwood, G A Navratil, R S Post, Phys.Fluids 20(1977) 148.

12. T Tomano. Conf. on Plasma Phys and Contr.Nucl.Fus.Res.Tokyo, 2 (1973) 97.

13. T Tomano. Phys.Rev.Lett 30 (1973) 431.

14. J Sinnis, M Okabayashi, J Schmidt, S Yoshikawa, Phys.Rev.Lett.29(1972) 1214.

15. S Yoshikawa, Phys.Fluids 13 (1970) 2300.

16. M Okabayashi, J Schmidt, J Sinnis, S Yoshikawa, Contr.Fus.and Plasma Phys. Res.Grenoble Vol.I (1972) 92.

17. R P Freis, C W Hartman, F M Hamzeh, A J Lichtenberg, Nuclear Fusion 13 (1973) 533

18. S Skellett, VII Symp. on Fus.Technology,Grenoble (1972) 251.

19. J L Johnson, S von Goeler, Phys. Fluids 12 (1969) 255.

20. J Connor and J B Taylor, Nuclear Fusion 17 (1977) 1047.

21. E M Jones and C A Steed. Proc. DECUS Europe Symp.Copenhagen,Denmark. (1978) 453.

22. R F Ellis and R W Motley, Phys. Fluids 17 582 (1974).

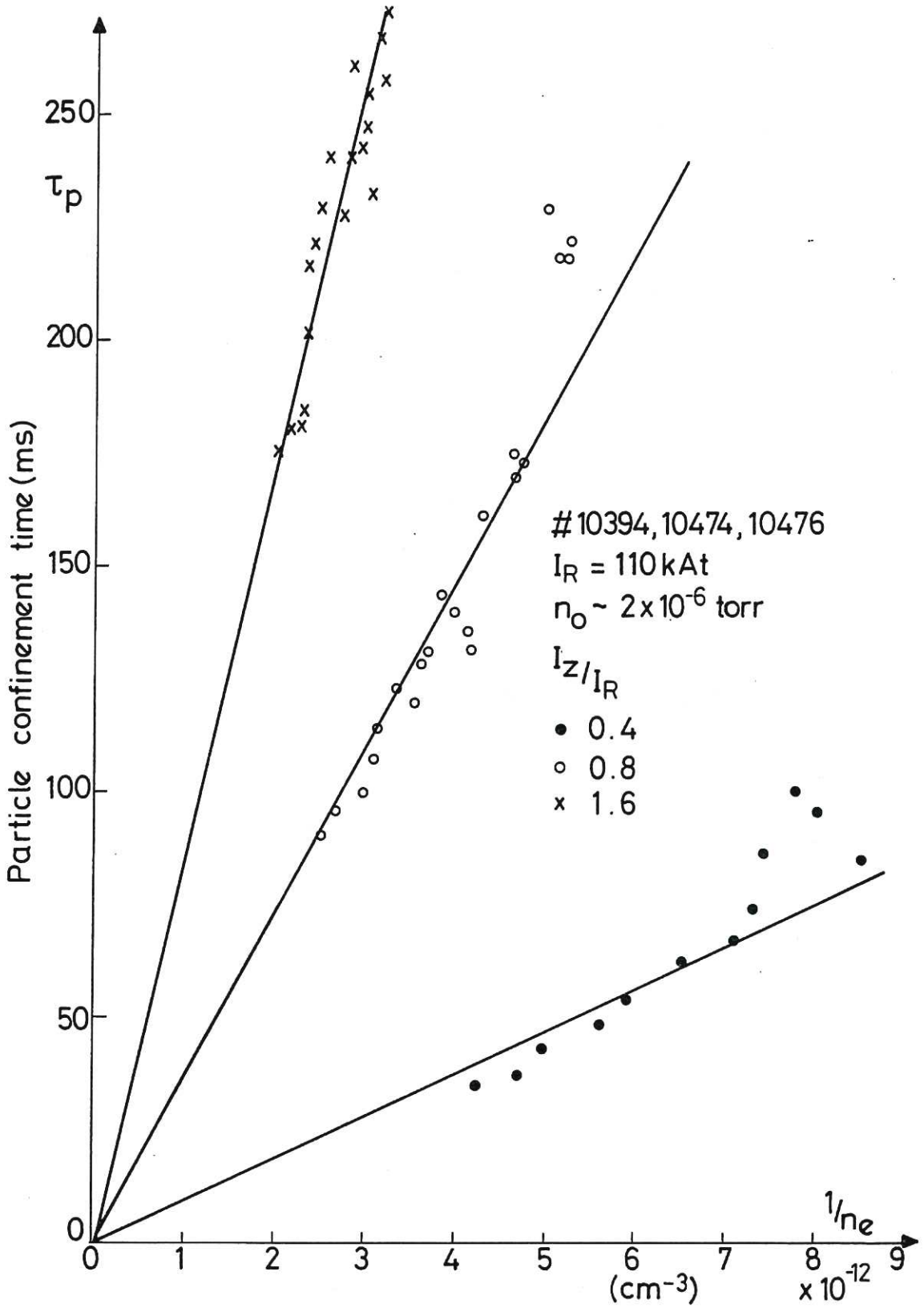

Fig. 1 Variation of particle confinement time with electron density at three different values of toroidal field.

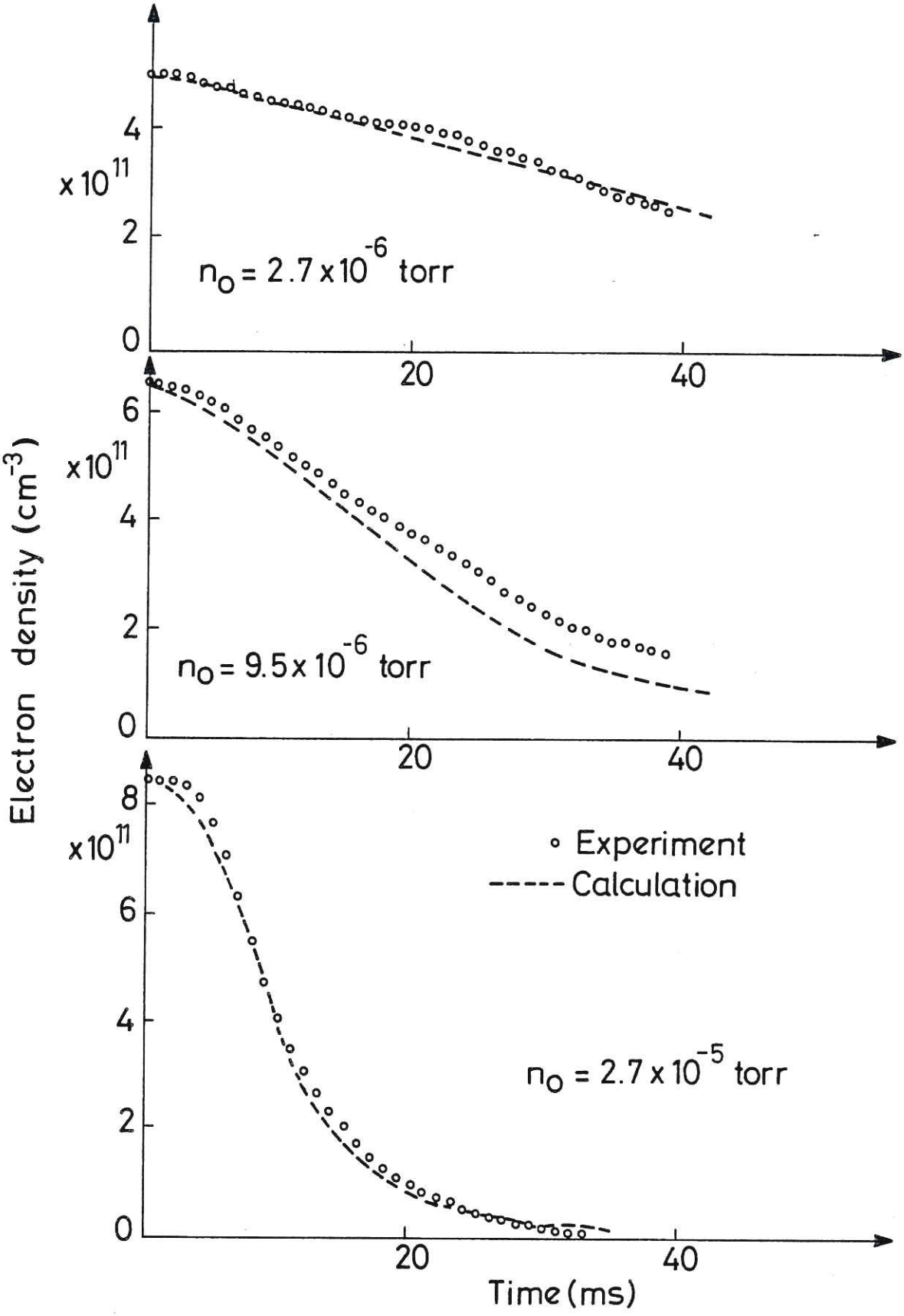

Fig. 2 Comparison of experimental and calculated electron density decay as a function of neutral gas density.

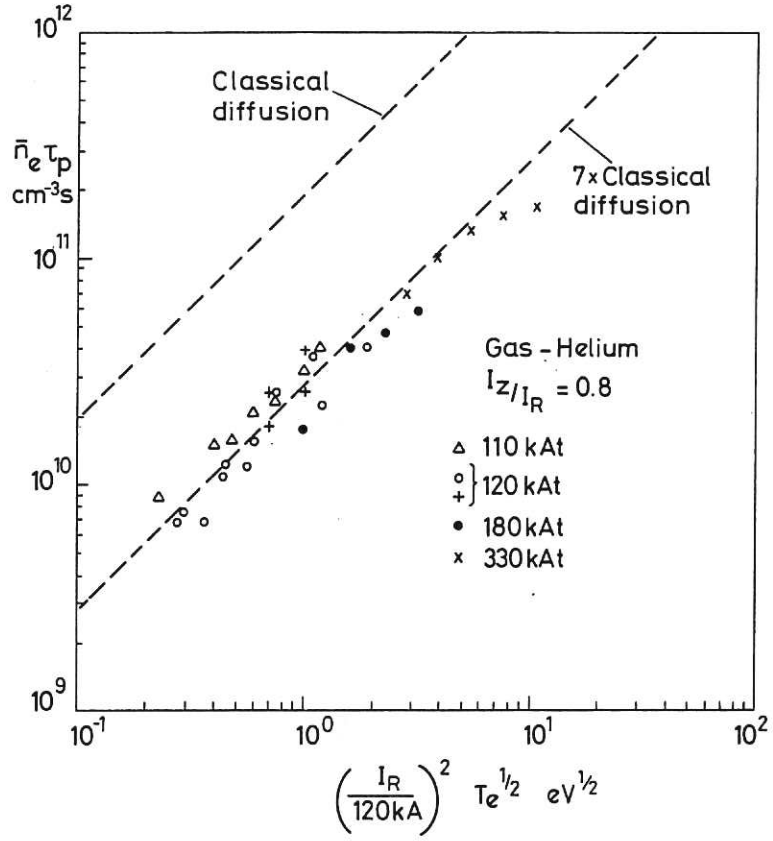

Fig. 3 Confinement time scaling with mean magnetic field strength.

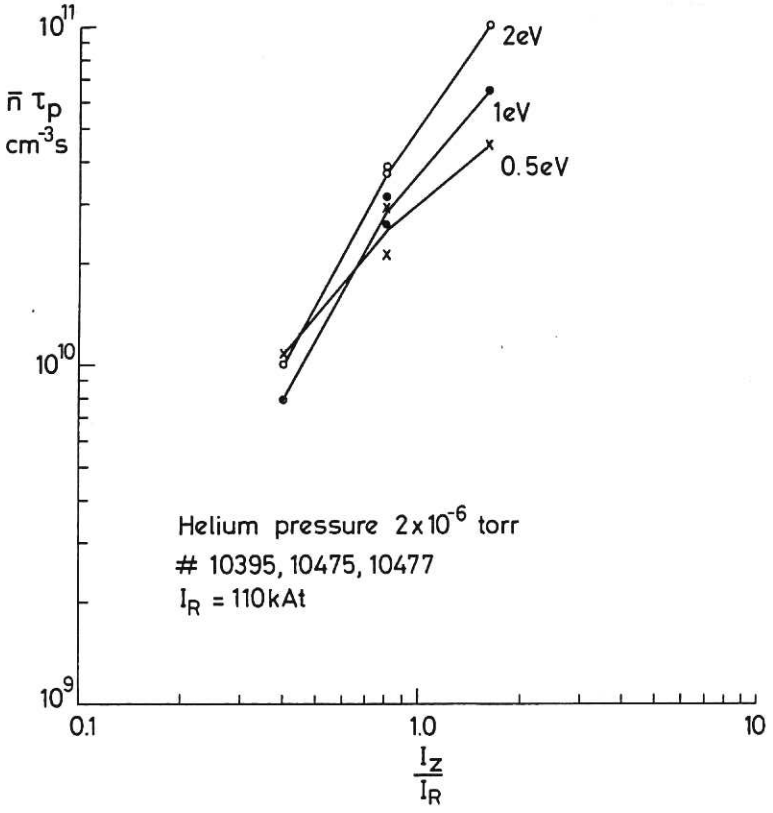

Fig. 4 Scaling of confinement time with magnetic shear in unheated decays.

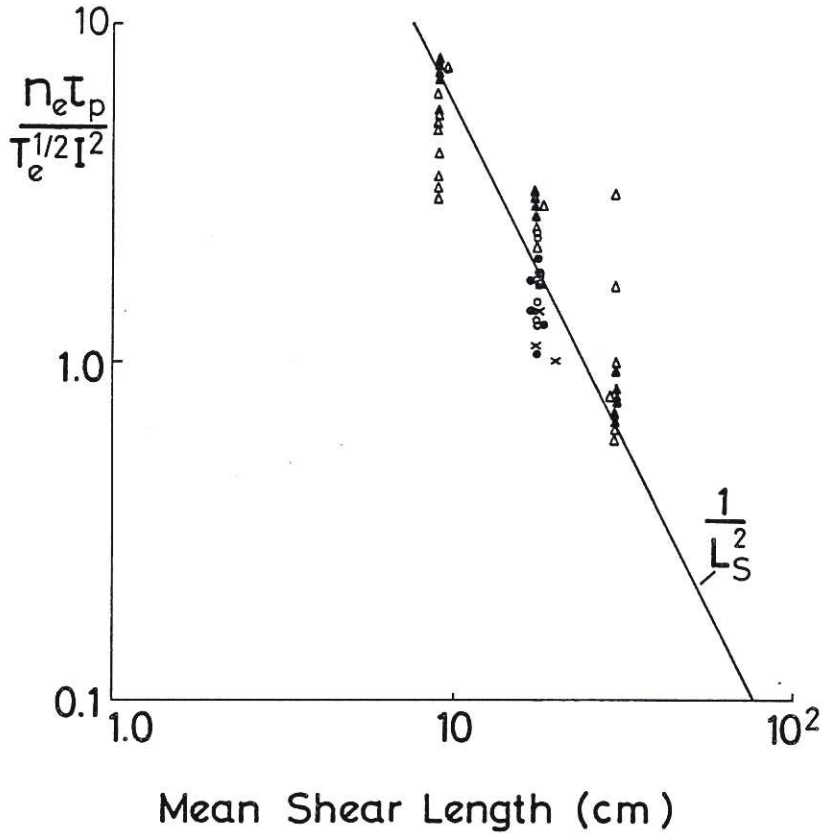

Fig. 5 Confinement time scaling with mean shear length L_S.

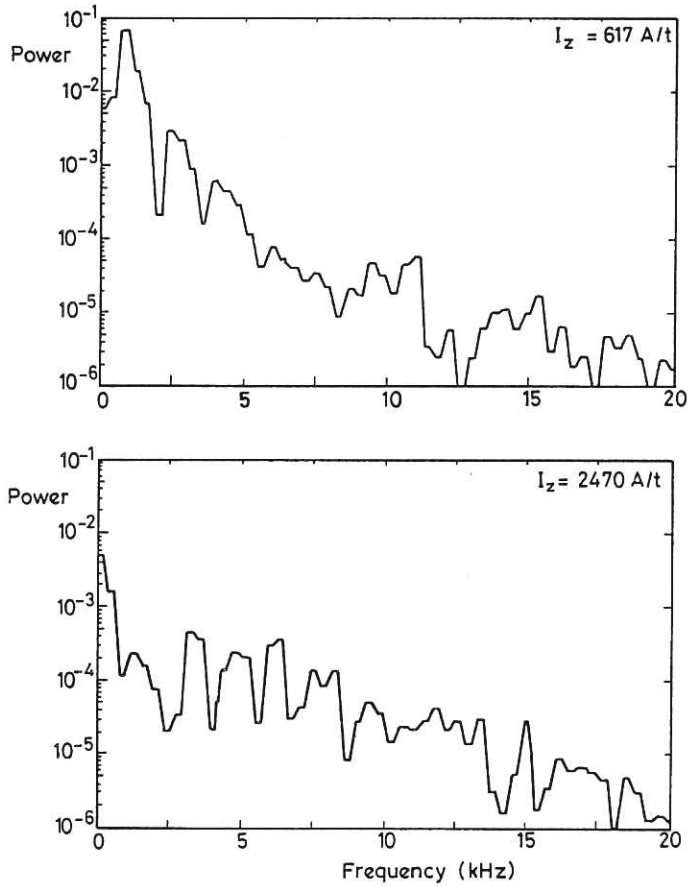

Fig. 6 Frequency spectra of potential fluctuations measured on axis at 3.25 cm from the ring surface.

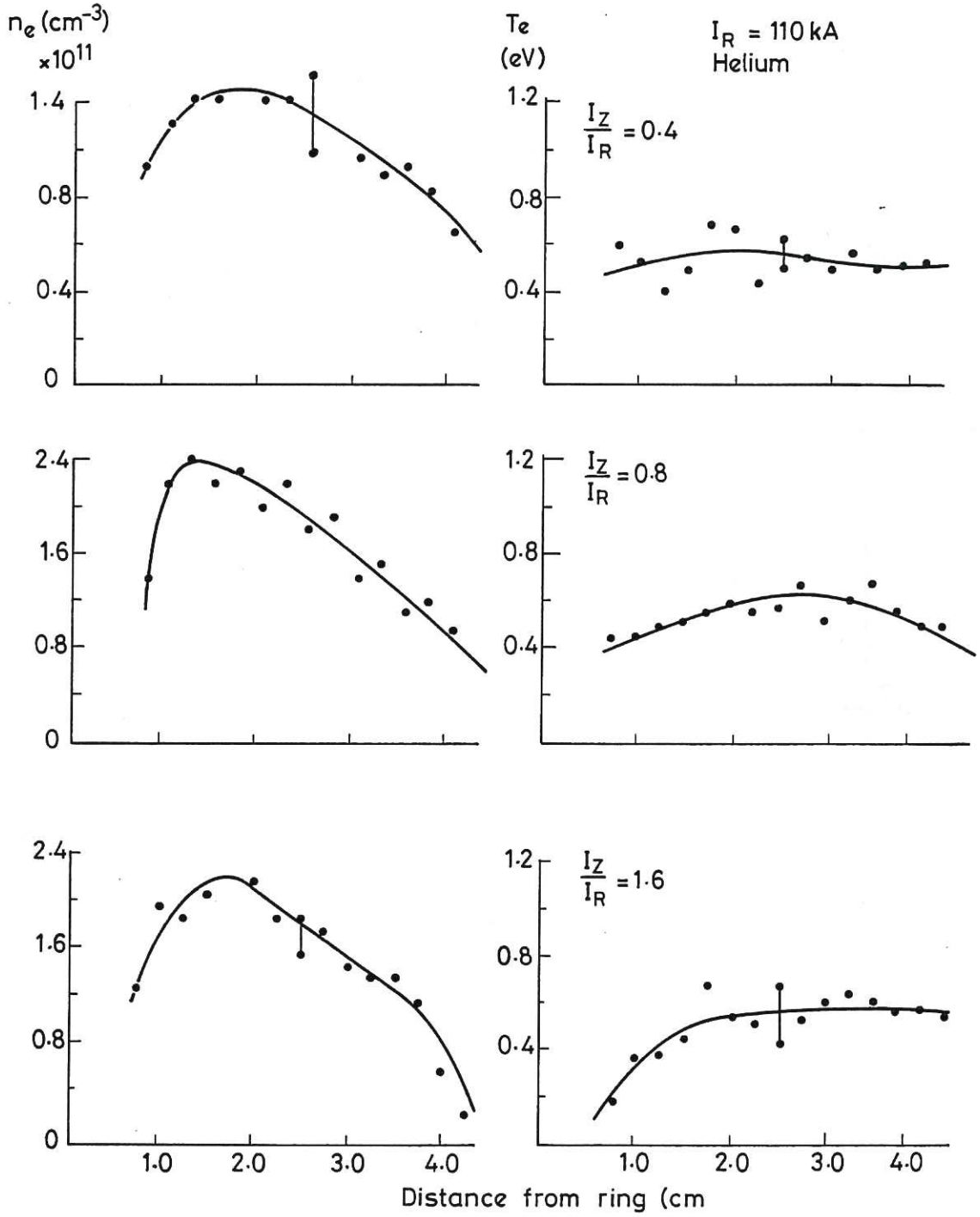

Fig. 7 Electron density and temperature profiles measured 25 msec after the main ECR heating is switched off.

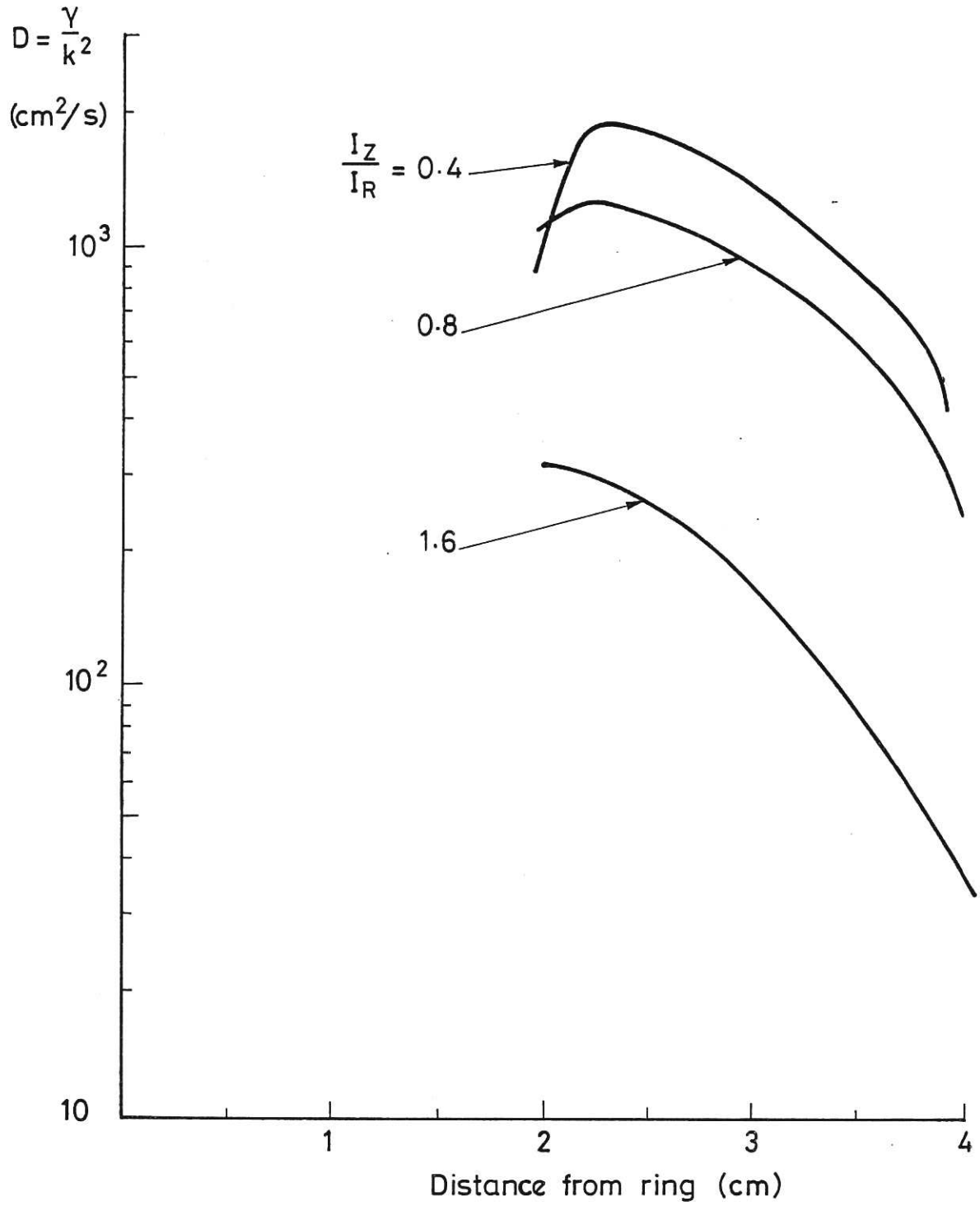

Fig. 8 Comparison of the quasi-linear diffusion coefficient γ/k_x^2 with the diffusion coefficient estimated from the decay rate of the mean electron density.